Korean J. Chem. Eng., 33(10), 2953-2960 (2016)
DOI: 10.1007/s11814-016-0137-z

pISSN: 0256-1115
eISSN: 1975-7220

Experimental investigation of nanofibrous poly(vinylidene fluoride) membranes for desalination through air gap membrane distillation process

Rasoul Moradi*, Javad Karimi-Sabet,†, Mojtaba Shariaty-niassar*,†, and Younes Amini*****

*Transport Phenomena & Nanotechnology Lab., School of Chemical Engineering, University College of Engineering, University of Tehran, Tehran, Iran
**NFCRS, Nuclear Science and Technology Research Institute, Tehran, Iran
***Department of Chemical Engineering, Isfahan University of Technology, Isfahan, Iran
(*Received 12 February 2016 • accepted 8 May 2016*)

Abstract−A comparative study was conducted to evaluate the performance of two membrane types of electrospun poly(vinylidene fluoride) (PVDF) and commercial ploytetrafluoroethylene (PTFE). The optimized needleless electrospinning technique was used to prepare PVDF membranes. Scanning electron microscopy (SEM), wettability tests, water flux, mechanical strength and liquid entry pressure (LEP) measurements were performed to evaluate the prepared membrane. Air gap membrane distillation (AGMD) experiments were carried out to investigate the salt rejection performance and the durability of membranes. The results show that our nanofibrous PVDF membrane presents higher water permeation flux (>20 kg/m^2 h) compared to commonly used PTFE. In addition, the experimental data confirms that competitive salt rejection efficiency (>99.8%) was obtained in this new membrane.

Keywords: AGMD, PVDF, Nanofibrous Membrane, Desalination, Needle-less Electrospinning

INTRODUCTION

Intensive population growth and global warming effect has intensified the demand for fresh water [1]. Hence, extensive researches have been focused to develop the efficient methods for producing good quality drinking water. Of these methods, desalination processes--removing salt from seawater and brackish water--are preferred as the main method for obtaining fresh water in arid regions.

Recently, membrane technology has been considered as the most cost/energy-effective desalination method compared to conventional distillation processes. In most membrane processes, the driving forces are hydrostatic pressure or chemical/electrical potential [2]. The well-known reverse osmosis (RO) is one of these isothermal membrane processes, which is commercialized for the desalination of seawater [3]. However, such membrane processes are not efficient for producing economized water and meeting the future huge demand. Therefore, developing new membrane processes for desalination of seawater is inevitable. Membrane distillation (MD) has attracted a great amount of research interest for possible substitute for RO in water desalination [3,4].

MD is a non-isothermal membrane operation in which the driving force is the partial vapor pressure difference across the porous and hydrophobic membrane [3-5]. In air gap configuration of MD (AGMD), a condensation surface is used inside the module, and an air gap is interposed between the membrane and the condensation surface in the permeate side of the module [6,7]. The mechanisms of AGMD mass transport across the membrane have been investigated in various studies [8-10]. Previous investigations have shown that membrane properties play the main role in the transport phenomena and efficiency of this process. For this reason, parameters such as pore size, pore size distribution, hydrophobicity, tortuosity, and thickness determine the final AGMD performance [11,12].

Improving porosity and decreasing of the membrane thickness both enhance the membrane permeation flux. However, these changes result in a decrease of the membrane's mechanical strength [13,14]. Membrane material, additives, production method and conditions are some of the most important parameters that directly influence the physico-chemical properties of the synthetic membrane and its separation performance. The conventional membranes of MD are commercial ploytetrafluoroethylene (PTFE) membranes originally fabricated for various separation processes like microfiltration. These commercial membranes have the main characteristics of MD membranes, such as high porosity, hydrophobicity and a greater lifetime [15,16]. However, the permeation flux and the separation efficiency of these microfiltration membranes are not in an appropriate range when they are used in the MD process. Thus, the preparation of the efficient MD specific membranes is the crucial subject for commercial MD process [17,18].

Poly(vinylidene fluoride) (PVDF) is another polymer intensively employed to produce MD membranes due to its low surface energy, high hydrophobicity, porosity and good stability [19]. These advantages ensure a high permeation flux in the MD process without interrupting other characteristics of the membrane such as mechanical properties and hydrophobicity [20,21].

Conventionally the main method of PVDF membrane fabrication is phase inversion technique. Recently, electrospinning has attracted attention for its versatility, flexibility and ability to produce nanofibrous films with large surface area to volume ratio [23-25].

†To whom correspondence should be addressed.
E-mail: j_karimi@alum.sharif.edu, mshariat@ut.ac.ir

With using electrospinning, the superior characteristics could be inducted into the membranes [26]. However, it is difficult to fabricate PTFE membranes by electrospinning due to non-polar characteristics of PTFE. In fact, it is insoluble in common solvents [27-29]. On the other hand, PVDF could be easily introduced into electrospinning to produce the nanofibrous membranes [30].

In the present work an experimental design for fabrication of electrospun PVDF membranes has been considered. One of our objectives was the investigation of the individual and mutual effects in the electrospinning variables (applied voltage and distance between the needle and the collector) on the diameter of the electrospun PVDF fibers. The synthesized membranes were characterized, and their applications in AGMD process were examined for desalination purposes. Finally, the performances of synthesized membranes were compared with the commercial PTFE membranes.

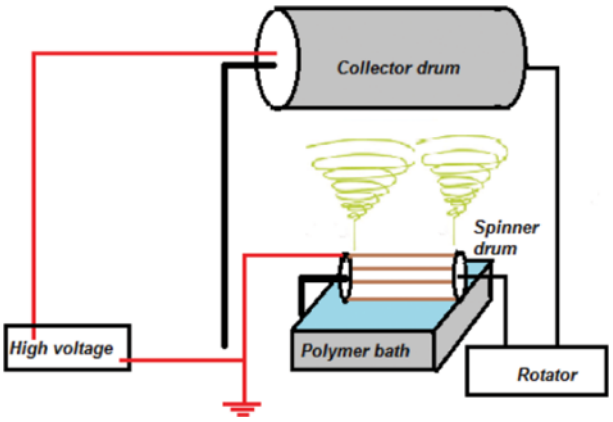

Fig. 1. Schematic of needle-less electrospinning setup used for producing nanofiber membranes.

EXPERIMENTAL SETUP

1. Materials

Poly(vinylidene fluoride), the polymer used in this work, was obtained from Sigma Aldrich, USA (PVDF synthesis grade with 400,000-600,000 molecular weights). Solvents of N, N-dimethylacetamid, (DMAc, synthesis grade, >99%), Acetone and methanol were from Merck, Darmstadt, Germany. NaCl was also purchased from Merck. Deionized double distilled water was used to prepare salty feed solutions in AGMD experiments. The commercial polytetrafluoroethylene membranes (PTFE-TF200) were purchased from Gelman, USA.

2. Membrane Preparation Method

In this study, PVDF nanofibrous membrane was fabricated through electrospinning technique. As represented in Fig. 2, needle-less roller electrospinning setup was used to increase the throughput of electrospinning [30]. Optimized electrospinning parameters were determined by a number of experiments in order to achieve better characteristics in the synthetic membrane. The roller and collector rotating speed were 2 and 200 rpm, respectively. As clearly depicted in Fig. 1, the roller spinneret was situated inside the precursor PVDF solution bath at 30 °C. PVDF solution of 10% (w/v) concentration was prepared in a mixture of DMAc and acetone at a ratio of 3 : 2. Before electrospinning, the prepared precursor solution was vigorously stirred for 1 h at 30 °C and then sonicated for 15 min.

3. Membrane Characterization Methods

Field emission scanning electron microscope (FESEM, F4160 and HITACHI, Japan) was used to observe the porous structure of synthetic PVDF and commercial PTFE membranes at an accelerating voltage of 30 kV. Water liquid entry pressure (LEP) tests were carried out for both types of membrane with a homemade setup. To investigate the hydrophobicity of the membranes, the sessile drop method was implemented in a goniometer (Data-Physics, OCA 20, Germany) to obtain water contact angles.

The mechanical properties of membranes were measured through a tensile testing machine (Instron 5982, MA, USA). This device was equipped with a 5 kN load cell and pneumatic grips, at a strain rate of 1mm/min. The size of the dog-bone shaped specimen's gauge length was 16 mm with a width of 3.3 mm. For every sample, at least four tests were repeated to ensure reproducibility.

4. Module Design and Construction

A flat-sheet module of 30 cm length and 15 cm width was fabricated. High-density PTFE materials were used in the module fabrication to maintain high thermal and mechanical stability for long time operations. In the designed module, the effective membrane area was about 5 cm×15 cm (75 cm^2).

5. AGMD Experiments

The schematic representation of the AGMD unit cell is shown

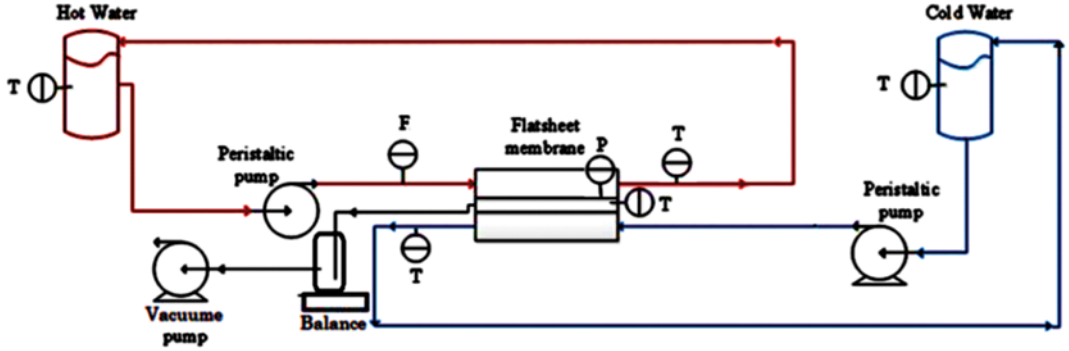

Fig. 2. Vacuum enhanced AGMD unit cell flow diagram used for $H_2{}^{18}O$ concentrating experiments. Blue and red colored streams represent the cooling and feed streams respectively.

Table 1. Operational parameters for AGMD unite cell experimentation using synthetic nano-fibrous PVDF and Commercial PTFE membranes. Both Feed and coolant streams were double distilled deionized water

Parameter	Value
Coolant temperature (°C)	20
Coolant flow rate (mL/min)	300
Feed flow rate (mL/min)	100
Air gap thickness (mm)	7
Air gap vacuum (kPa)	75
Membrane effective area (cm^2)	75

in Fig. 2. In the AGMD configuration, peristaltic pumps were employed to flow out the permeate stream, which caused a relative vacuum in the module air gap section (~75 kPa). Hence, we labeled this AGMD setup a vacuum enhanced AGMD. The feed and coolant stream temperature were stabilized at 65 °C and 20 °C, respectively. The MD experiments established the best compromise among different parameters such as permeate flux and separation efficiency. The optimized values of temperatures, flow rates and pressures were applied in all AGMD experimentations. The operational parameters are listed in Table 1.

RESULTS AND DISCUSSION

1. Membrane Preparation

The fiber diameters are crucial for producing a membrane with efficient MD performance. In fact, the mechanical strength and permeability of membranes are highly influenced by the fiber mean diameter. In addition, the polymer concentration affects the prepared nanofibers diameters. The influence of the PVDF concentration on produced fiber diameters is illustrated in Fig. 3(a). The figure clearly shows that a noticeable increase occurs in the fiber diameters with PVDF concentration in precursor solution. For PVDF weight ratio of 10 wt%, the fiber diameters were around 200 nm, while the achieved fiber diameters were greater than 400 nm in the concentrations above than 15 wt%.

In large-scale membrane production process, productivity is an important factor in the electrospinning method. As depicted in Fig. 3(a), the electrospinning productivity also increases with the PVDF concentration in the precursor solution. For weight ratio of 10 wt%, the achieved productivity was about 5, which was suitable for our laboratory demands. Therefore, 10 wt% of PVDF polymer solution was chosen for producing nanofibers with favorable diameters (250±150 nm). Fig. 3(b) illustrates effects of both PVDF concentration and collector-electrode distance on the applied voltage threshold in electrospinning experiments. As shown in the plot, the threshold voltage is increased by the PVDF concentration as well as collector-electrode distance.

Fig. 3(c) illustrates the variation of running time and fiber diameters with applied voltage. It is obvious that the electric field strength is reduced in the electrospinning zone when the collecting distance increases. As this parameter increases, a higher voltage is needed to conduct stable electrospinning. It is clear that both mentioned parameters result in higher thresholds of applied voltage. Otherwise, the thick fibers were formed when the PVDF concentration and collector-electrode distance were increased at a constant voltage. It was found that the applied voltage and collecting distance must be 45 kV and 18 cm for preparation of the desired PVDF nanofiber membrane with appropriate fiber diameters, respectively. In this condition, the productivity value of about 5 could be achieved for the electrospinning process. In this system, the negative high voltage terminal is connected to a conductive drum covered by the aluminum foil as the collector of fibers.

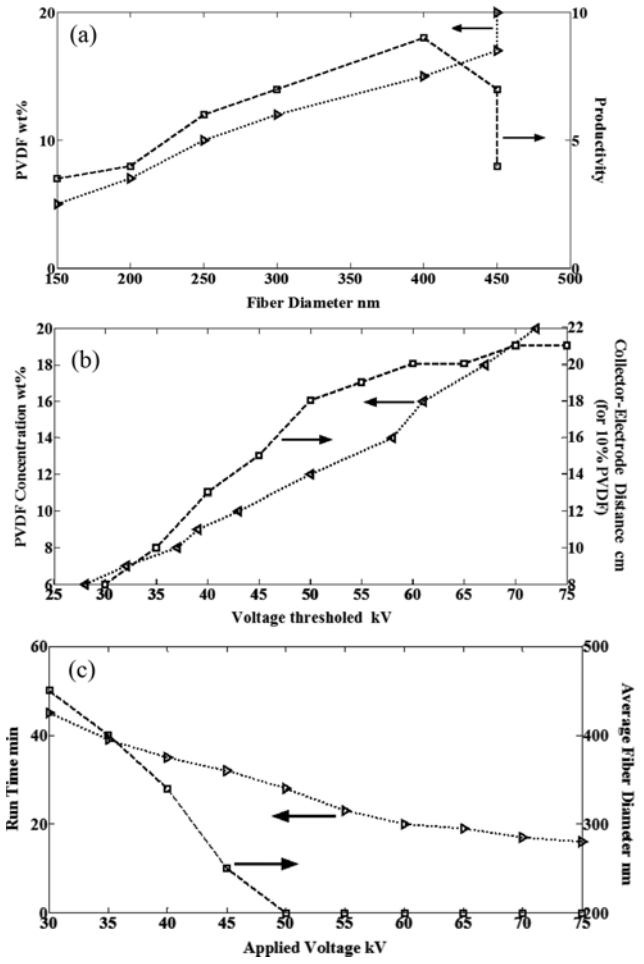

Fig. 3. Electrospinning parameter optimazations: (a) The effect of PVDF concentration in precursor solution on the prapared fiber diameter and electrospinning productivity. (b) Variations of the applied voltage thresholeds with PVDF weight ratio and collector-electrod distance. (c) The influence of applied voltage changes on the needed running time and the diameters of produced fibers.

2. Membrane Properties

Membrane properties have significant effects on the membrane desalination process. Hence, the prepared membranes were characterized to evaluate the role of the surface hydrophobicity and morphology on the membrane performance. The water contact angles of the membranes were determined to investigate the hydrophobicity level. The measured contact angle of the synthetic PVDF membrane was θ=131°, which was slightly greater than the value of θ=124° for PTFE membrane. This difference may be attributed to

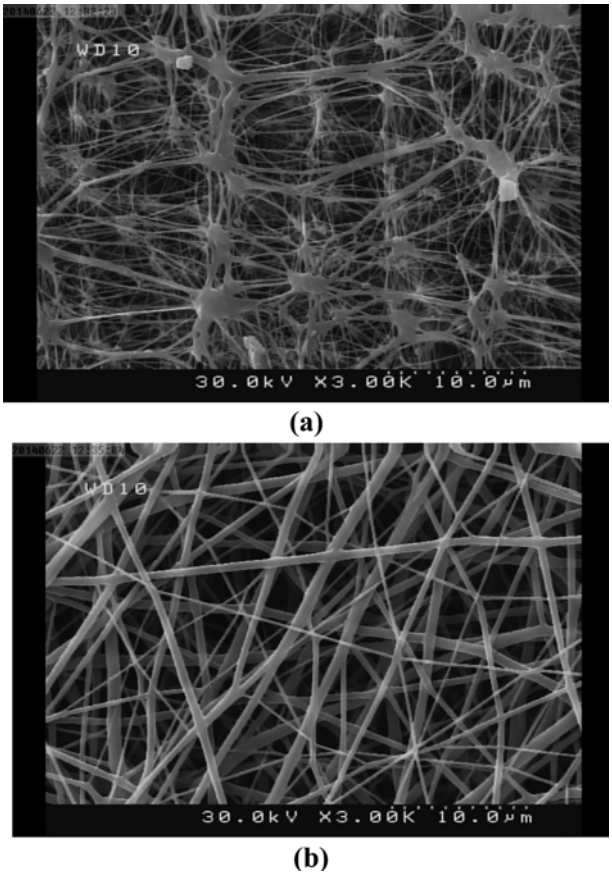

Fig. 4. FESEM images of (a) PTFE membrane, and (b) synthetic PVDF membrane, respectively.

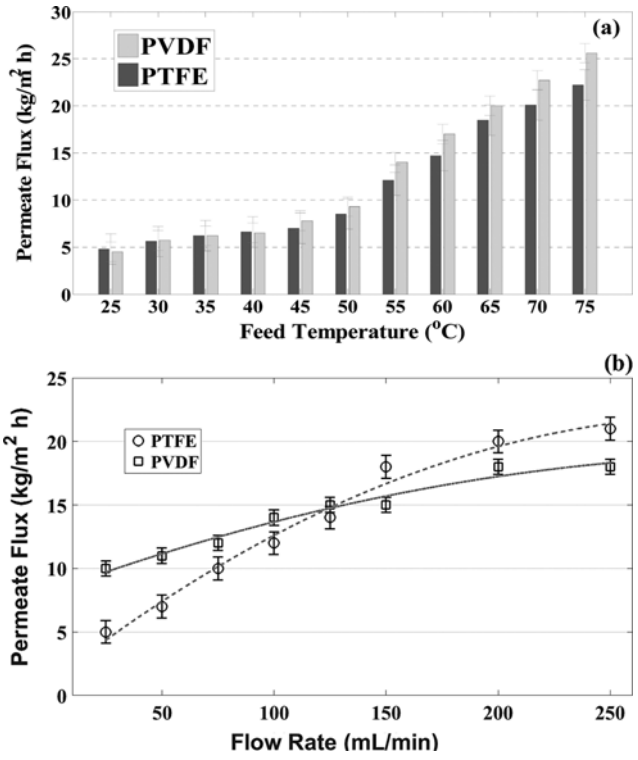

Fig. 5. Permeate flux changes as a function of (a) applied temperature gradient across the membrane, and (b) the applied feed flow rate, for both PVDF and PTFE membranes.

the nanofibrous structure with higher surface roughness of the electrospun PVDF membranes, while the reported contact angle is around 85° for non-fibrous PVDF membranes [31-33].

FESEM tests were performed to compare the morphological differences between non-fibrous PTFE and nanofibrous PVDF membranes. The obtained images are illustrated in Fig. 4(a) and 4(b). The figures clearly show that the nonwoven forms of the electrospun PVDF fibers produce intersected pores with greater tortuosity. However, comparison of these membranes shows that PTFE membranes contain island-like fractional parts and nodes, which are formed by biaxial stretching operations during their producing process. These nodes affect the surface characteristics and the separation ability of the PTFE membranes. The surface area occupied by key micro structural features also was estimated through SEM micrographs.

As illustrated in Fig. 4(a), the stretched fiber diameters of PTFE membranes are in a wide range from 50 nm up to a few micrometers. However, the synthesized PVDF fiber diameters range from 200 nm to 450 nm. This wide range affects the tortuosity and permeability of the membranes. Moreover, the thin fibers were fragile and easily ruptured under mechanical or thermal stress, and other membrane properties such as a mechanical strength are consequently affected by the fiber thicknesses. From mechanical strength aspects, PTFE membrane possesses higher tensile strength and Young's modulus in comparison with prepared PVDF membranes (Table 2). However, the mechanical strength rarely affects the membrane performance in a clear manner, as the operational pressure is low in the AGMD process, [34]. Otherwise, membrane durability becomes an important issue for large-scale and long-term MD operations [35].

Furthermore, the pore sizes max and min values for PVDF (~470 nm and ~220 nm respectively) were found to be higher than PTFE pore sizes (~350 nm and ~150 nm, respectively). This means that the prepared PVDF membrane has a wide pore size distribution. Moreover, the greater pore sizes of the PVDF membrane cause higher permeate flux in AGMD experiments. The increasing of the permeation flux led to loss of separation efficiency of PVDF

Table 2. Measured values of pore size, porosity, water contact angle, thickness, LEP and mechanical strength for the PTFE and PVDF membranes at ambient conditions

Membrane	Type	δ (μm)	d_p (μm)	d_{min} (μm)	d_{max} (μm)	ε (%)	LEP (kPa)	θ (°)	Young's modulus (MPa)	Tensile strength (MPa)
PTFE/PP (TF200)	Commercial	178	0.200	0.150	0.350	75	260	124	74.2±7.5	8.5±2.5
PVDF/PP	Synthetic	150	0.250	0.220	0.470	85	275	131	54.5±7.5	4.2±2.5

membrane compared to PTFE membrane.

Fig. 5(a) shows the variation of the membrane permeation flux with respect to the applied feed temperature. These results indicate that the PVDF membrane permeability significantly is increased with the feed temperature compared to PTFE membranes. For PTFE membranes at temperatures less than 40 °C, permeate flux is likely higher than PVDF membranes. However, PVDF permeation flux increases more than PTFE membranes for temperatures greater than 40 °C. Although permeation flux increasing is an important operational parameter, some side effects such as a decreasing in the separation efficiency are observed in the process.

The increasing of the temperature difference between the hot feed and the cooling streams) shows that the water permeation flux for both membranes follows the same trends. However, the primitive values of PVDF for the permeation flux and the rate of increase are both higher than for PTFE membranes. This is because of some characteristics of synthetic PVDF membranes, such as higher porosity and less thickness (from Table 2). In fact, the high membrane permeation strongly affects the salt rejection performance in AGMD experiments. It is concluded that the desired temperature gradient across the membrane (between the hot and cold streams) is about 45 °C. Since the cooling stream's temperature was stabilized at 20 °C for all AGMD experiments, the hot feed temperature was fixed at 65 °C. In this situation, actual temperature recorded on the cold side surface of the membrane was measured to be about 4-5 °C warmer than the cold stream (about 24-25 °C). This is due to the applied distance between the membrane surface and the cooling aluminum sheet in the air gap of membrane module. In addition, membrane heat conductivity intensifies this undesirable effect.

To evaluate the effect of feed flow rate on the permeate flux, a series of AGMD experiments were conducted with various feed flow rates at the same operating temperature. Fig. 5(b) represents the permeation fluxes obtained for both types of membranes. The results indicate that the permeation flux increases with feed flow rate for both types of membranes. However, PTFE membranes experiences a steeper increase in permeation flux than synthetic PVDF membrane due to their lower LEP values. This means that the feed stream hydrostatic pressures increases as flow rates are raised. In fact, this occurs due to pore wetting and liquid diffusion through the membrane at higher flow rates. The liquid diffusion augments when the applied hydrostatic pressure is larger than membrane specific LEP values.

Dynamic contact angle results indicate that there is no significant change in the wettability property of the membranes over the time. This confirms the stability of the membrane surface properties from the hydrophobicity point of view. Higher water contact angle demonstrates that the nanofibrous PVDF membrane has greater pore wetting resistance than the commercial PTFE membranes. This directly influences the LEP data. LEP values should be greater than the hydrostatic pressure and the pressure difference at the membrane liquid/vapor interface to prevent pore wetting in MD processes [36,37].

Fig. 6 shows the variation of LEP with applied feed (pure water) temperatures for the main AGMD experiments. As shown, LEP is notably temperature dependent, and it experiences a drastic decrease with temperature increasing. LEP values for both types of membranes were higher than the operational pressure difference (100-150 kPa) in AGMD experiments. Based on the experimental results, LEP decreases for both PVDF and PTFE membranes when the applied feed temperature increases. Nevertheless, PTFE membrane experiences a greater decrease at low temperatures (<55 °C) as the water temperature increases. In contrast, the obtained reduction trend at high temperatures (>55 °C) is sharper for PVDF. In addition, at 70 °C LEP value of PTFE (~170 kPa) is greater than PVDF (~160 kPa). With increasing in the feed temperature the pore structure of PVDF membrane is more affected compared to PTFE. It seems that PVDF experiences a collapse in pore shape and structure at temperatures higher than about 55 °C. This results in rapid pore wetting occurrence for PVDF rather than PTFE. In fact, PVDF is more sensible to higher temperature, and its surface properties and morphology likely tend to deform at high temperatures. LEP and water contact angle results imply that PVDF fibrous structure is the key factor in determining the membrane wetting resistance and hydrophobicity. The island-like fractional parts and nodes led to decrease in the porosity and tortuosity of the PTFE membrane. This results in decreasing of the membrane hydrophobicity as well as LEP values. In contrast, PVDF nanofibrous structure provides slightly higher hydrophobicity and porosity of the prepared membrane.

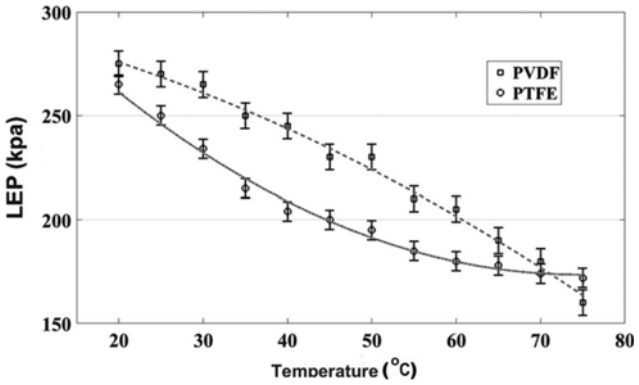

Fig. 6. Variation of LEP values as a function of feed temperature for both types of membranes.

One of the problems in the MD process is the presence of air in the membrane pores. The air inside the pores hinders the mass transfer, which decreases the permeation flux [11]. In our work, their effects were diminished through applying a relative vacuum by using the pump primarily utilized for permeate collecting. Previous studies pointed out that membrane short durability as well as low permeation flux are problems that prevent the implementation of the MD process in large-scale [11,12].

In the absence of air in membrane pores, applying a relative vacuum caused the flow of the water vapor through the pores of membrane to assume a Knudsen flow type, but in the presence of air inside the pores at the same temperature range, the water vapor flow should be treated as a molecular flow.

3. AGMD Experiments

3-1. Effect of Feed Salt Concentration

In this section, effects of feed salt content on salt rejection efficiency of the membranes were performed in a series of AGMD

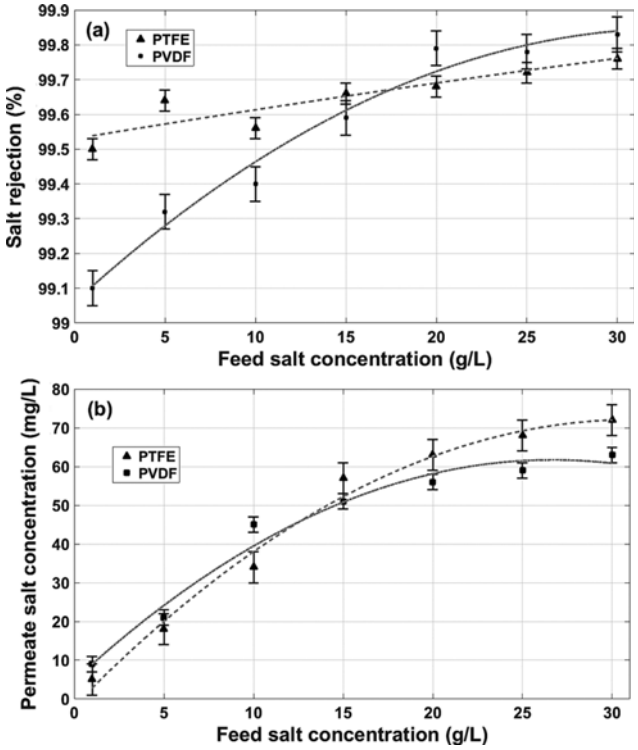

Fig. 7. Results of AGMD experiments for prepared salty as feed: (a) Variation of membrane salt rejection performance, and (b) variation of membrane permeate flux, as a function of applied feed salt concentration.

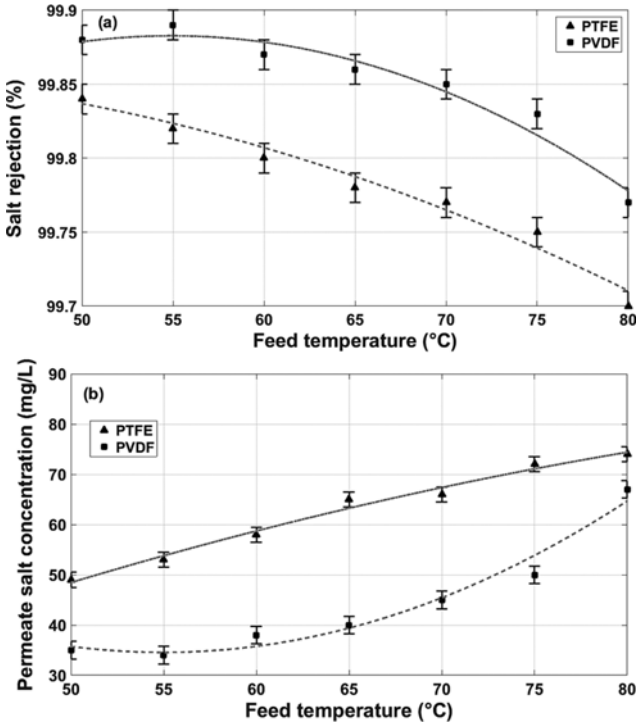

Fig. 8. Results of AGMD experiments with using salty water (25 g/L of NaCl) as feed (a) variation of membranes salt rejection performance, and (b) variation of membrane permeate flux, as a function of applied feed temperature.

experiments to evaluate the membranes performance in different salt concentrations. These experiments were carried out with feed inlet temperature of 70 °C and feed flow rate of 100 ml/min. The salt rejection efficiencies and permeate salt concentrations are shown in Fig. 9 for both types of membranes. As shown in Fig. 7(a), the performance of salt rejection is increased when the salt concentration is raised in the feed stream. However, the observed salt rejection of PVDF membrane is sharper than PTFE. In fact, this increasing in the salt rejection percent could not be attributed to the membrane better performance in high concentrations. To better evaluate the membrane performance in high feed concentrations, variations of the permeate salt concentration as a function of feed concentration were obtained and the results are exhibited in Fig. 7(b). This figure reveals that the permeated salt increases with feed salt concentration. However, the nanofibrous PVDF membranes exhibit better performance compared to commercial PTFE membranes at high salt concentrations (>15 g/L).

Moreover, Fig. 7(a) shows that at feed salt concentration below 15 g/L the PTFE membrane performs better in salt rejection. This result seems to indicate that in low salt concentration the rate of salt precipitation and fouling effects on the membrane surface is low. In addition, the probability of salt permeation through the membrane pores is negligible. In the other words, the membrane-based factors of both membranes do not affect the separation performance strongly. On the other hand, at high salt concentrations, the membranes play an important role in determining the separation performance. As mentioned earlier, PVDF membrane exhibits desired characteristics such as high LEP values and is expected to display high resistance to salt permeation in high concentrations. Therefore, we employed high salt concentrations to judge the salt rejection efficiency of the membranes. However, at low salt concentration PTFE membranes perform better because at this level of concentrations the salt permeation phenomena through the membrane pores are not dominant.

3-2. Effect of Feed Temperature

The influence of the feed temperature on salt rejection performance is illustrated in Fig. 8(a). The applied feed concentrations in AGMD experiments were 25 g/L. It can be found that the feed temperature clearly influences the performance of membrane desalination. As the feed temperature is increased, the salt rejection decreases for both types of membranes. It can be attributed to the decline of membrane separation efficiency at high feed temperatures. The salt concentration of permeation is shown as a function of feed temperature in Fig. 8(b), which indicates that the salt concentration in the permeate stream increases with feed temperature for both types of membranes. However, this increasing is intensive in the case of PVDF membranes. This observation shows that the nanofibrous PVDF membrane is more sensitive to the temperature, and its performance in the feed high temperatures diminished rapidly compared to PTFE membrane. This difference in variations is related to various intrinsic properties of polymers.

3-3. Natural Seawater Application

The natural seawater sample containing 27 g/L of NaCl was treated through AGMD experiments with synthetic and commercial membranes. The feed temperature and flow rate in all experi-

ments were fixed at 50 °C and 100 ml/min, respectively.

The direct application of the seawater as feed for AGMD process resulted in a prompt decline of the permeate flux. Results indicate that both membranes permeate is linearly decreasing with elapsed time for 75 hours. Indeed, it is mainly due to deposition of low soluble carbonate salts on the surface of membranes. The heating of feed causes the conversion of bicarbonate ions to carbonate ions. Then, the high scale deposition of salts with limited solubility such as $CaCO_3$ takes place and the fouling of the membranes pores occurs. Fig. 9 shows that the permeate conductivity is increased during the experiments for both membranes. This observation is due to salt permeation through the membrane pores by elapsed time. The comparison of long-term performance between two membranes shows that the permeate conductivity of nanofibrous PVDF membrane slightly increases compared to PTFE. The obtained increasing trend for PTFE membrane is considerable when seawater is applied.

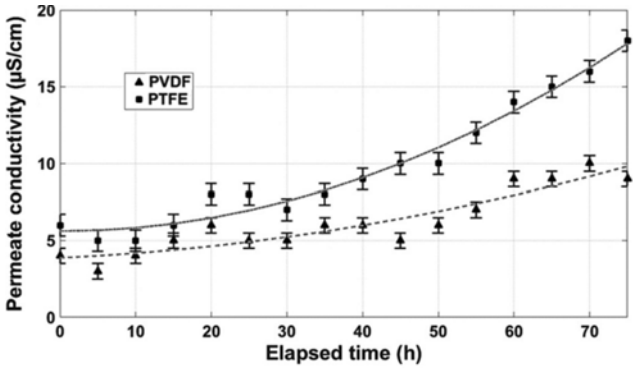

Fig. 9. Variation of permeate conductivity during continues 75 h of AGMD process for desalination of natural seawater.

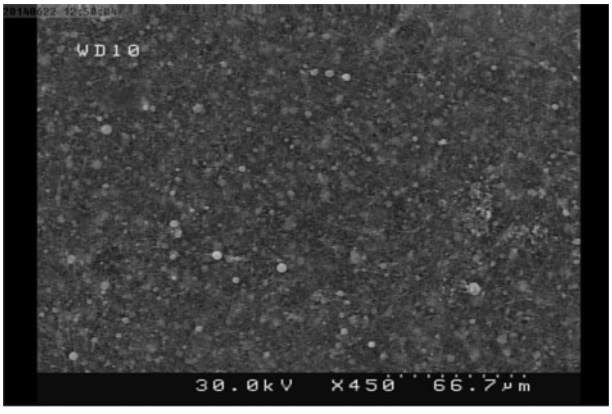

(a)

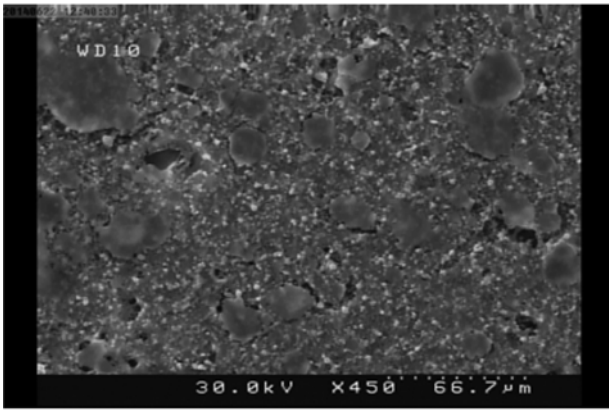

(b)

Fig. 10. FESEM images of the after-used (a) PVDF and (b) PTFE membrane.

Fig. 10 represents the FESEM images of membranes after subjecting to natural water in AGMD experiments. As shown, salt precipitation occurred on the surface of both membranes. However, it is obvious that the fouling in the case of PTFE membrane is considerable compared to PVDF membrane. This is due to the island-like structure of the PTFE surface, which enhances the nucleation and growth of perception components. As a result, after 50 hours of AGMD experiment, $CaCO_3$ precipitation on the PTFE membrane surface as the main fouling factor declines the flux to about half of its initial value. However, for the synthesized PVDF membrane this amount of flux reduction occurred after about 75 hours.

CONCLUSION

A comparative evaluation of the MD performance for both PVDF synthetic nanofibrous membranes and PTFE none-fibrous membranes was experimentally performed. The results of the MD single cell separation process indicate that the PVDF nanofibrous membrane has competitive salt rejection efficiency in AGMD experiments. Indeed, PVDF synthetic membranes exhibited higher salt rejection performances of above 99.8% when high salt concentrations (>20 g/L) were applied. Furthermore, AGMD experiments with using feed of natural seawater demonstrated that PVDF membrane was more resistive to fouling effects and exhibited dominant operative performance. The AGMD permeate flux declined more slowly for PVDF membrane compared to that of PTFE membrane. However, the low durability results in poor desalination efficiency during the long-term processes when synthesized PVDF membranes are used. Finally, the results of permeate conductivity test prove that commercial PTFE membrane has high salt rejection ability in long-term AGMD experiments.

REFERENCES

1. E. El-Zanati and K.M. El-Khatib, *Desalination*, **205**, 15 (2007).
2. Y. Xu, B. K. Zhu and Y. Y. Xu, *Desalination*, **189**, 165 (2006).
3. M. Gryta, M. Tomaszewska, J. Grzechulska and A. W. Morawski, *J. Membr. Sci.*, **181**, 279 (2001).
4. M. Hofman-Bieniek, K. Jasiewicz and R. Pietrzak, *Korean J. Chem. Eng.*, **31**, 304 (2014).
5. K. W. Lawson and D. R. Lloyd, *J. Membr. Sci.*, **124**, 1 (1997).
6. M. S. El-Bourawi, Z. Ding, R. Ma and M. Khayet, *J. Membr. Sci.*, **285**, 4 (2006).
7. T. Y. Cath, V. D. Adams and A. E. Childress, *J. Membr. Sci.*, **228**, 5 (2004).
8. M. A. Izquierdo-Gil, M. C. Garcıa-Payo and C. Fernandez-Pineda,

J. Membr. Sci., **155**, 291 (1999).
9. W. J. Koros, Y. H. Ma and T. Shimadzu, *J. Membr. Sci.*, **120**, 149 (1996).
10. C. M. Guijt, G. W. Meindersma, T. Reith and A. B. Haan, *Sep. Purif. Technol.*, **43**, 233 (2005).
11. R. W. Schofield, A. G. Fane, C. J. D. Fell and R. Macoun, *Desalination*, **77**, 279 (1990).
12. R. W. Schofield, A. G. Fane and C. J. D. Fell, *J. Membr. Sci.*, **53**, 159 (1990).
13. T. Uragami, M. Fujimoto and M. Sugihara, *Desalination*, **34**, 311 (1980).
14. M. Khayet, C. Y. Feng, K. C. Khulbe and T. Matsuura, *Polymer*, **43**, 2879 (2002).
15. M. Mulder, *Basic principles of membrane technology*, First Ed., Kluwer Academic Publishers, Dordrecht (1996).
16. R. Moradi, J. Karimi-Sabet, M. Shariaty-Niassar and Y. Amini, *Chem. Eng. Process.*, **100**, 26 (2016).
17. R. Moradi, J. Karimi-Sabet, M. Shariaty-Niassar and M. A. Koochaki, *Polymers*, **7**, 1444 (2015).
18. Z. M. Huang, Y. Z. Zhang, M. Kotaki and S. Ramakrishna, *Comp. Sci. Technol.*, **63**, 2223 (2003).
19. C. Y. Feng, K. C. Khulbe, T. Matsuura, R. Gopal, S. Kaur, S. Ramakrishna and M. Khayet, *J. Membr. Sci.*, **311**, 1 (2008).
20. D. Wu, X. Huang, X. Lai, D. Sun and L. Lin, *J. Nanosci.*, **10**, 4221 (2010).
21. H. Niu, T. Lin and X. Wang, *J. Appl. Polym. Sci.*, **114**, 3524 (2009).
22. F. Liu, N. A. Hashim, Y. Liu, M. R. Moghareh Abed and K. Li, *J. Membr. Sci.*, **375**, 1 (2011).
23. Y. Ma, Y. Su, Y. Li and Zh. Jiang, *Korean J. Chem. Eng.*, **32**(9), 1902 (2015).
24. Z. D. Hendren, J. Brant and M. R. Wiesner, *J. Membr. Sci.*, **331**, 1 (2009).
25. M. Essalhi and M. Khayet, *J. Membr. Sci.*, **433**, 167 (2013).
26. M. Mulder, *Basic principles of membrane technology*, First Ed., Kluwer Academic Publishers, Dordrecht (1996).
27. H. Fan and Y. Peng, *Chem. Eng. Sci.*, **79**, 94 (2012).
28. J. Phattaranawik, R. Jiraratananon and A. G. Fane, *J. Membr. Sci.*, **215**, 75 (2003).
29. D. Y. Cheng and S. J. Wiersma, US Patent, 4,419,242 (1983).
30. H. Niu, T. Lin and X. Wang, *J. Appl. Polym. Sci.*, **114**, 3524 (2009).
31. Y. Fujii, S. Kigoshi, H. Iwatani, M. Aoyama and Y. Fusaoka, *J. Membr. Sci.*, **72**, 73 (1992).
32. C. Feng, K. C. Khulbe, T. Matsuura, R. Gopal, S. Kaur, S. Ramakrishna and M. Khayet, *J. Membr. Sci.*, **311**, 1 (2008).
33. C. Burger, B. S. Hsiao and B. Chu, *Ann. Rev. Mater. Res.*, **36**, 333 (2006).
34. Z. Z. Zhao, J. Q. Li, X. Y. Yuan, X. Li, Y. Y. Zhang and J. Sheng, *J. Appl. Polym. Sci.*, **97**, 466 (2005).
35. R. Wang, Y. Liu, B. Li, B. S. Hsiao and B. Chu, *J. Membr. Sci.*, **392**, 167 (2012).
36. M. Essalhi and M. Khayet, *J. Membr. Sci.*, **433**, 167 (2013).
37. Y. Fujii, S. Kigoshi, H. Iwatani and M. Aoyama, *J. Membr. Sci.*, **72**, 53 (1992).